

Human Zw10 and ROD are mitotic checkpoint proteins that bind to kinetochores

G.K.T. Chan*, S.A. Jablonski*, D. A. Starr†‡, M.L. Goldberg† T. J. Yen*§

*Fox Chase Cancer Center, 7701 Burholme Avenue, Philadelphia, Pennsylvania 19111, USA

†Department of Molecular Biology and Genetics, Cornell University, Ithaca, New York 14853, USA

‡Current address: Department of Molecular, Cellular and Developmental Biology, University of Colorado, Boulder, Colorado 80309, USA

Se-mail: tj_yen@fcc.edu

Here we show that human Zeste White 10 (Zw10) and Rough deal (Rod) are new components of the mitotic checkpoint, as cells lacking these proteins at kinetochores fail to arrest in mitosis when exposed to microtubule inhibitors. Checkpoint failure and premature mitotic exit may explain why cells defective for hZw10 and hRod divide with lagging chromosomes. As Zw10 and Rod are not conserved in yeast, our data, combined with an accompanying study of *Drosophila* Zw10 and Rod, indicate that metazoans may require an elaborate spindle checkpoint to monitor complex kinetochore functions.

The mitotic checkpoint prevents cells with unaligned chromosomes from prematurely exiting mitosis^{1,2}. The mitotic checkpoint in budding yeast relies on Mad1, 2 and 3, Bub1, 2 and 3 and Mps1 (refs 3–5). The discovery of metazoan orthologues of Mad1 (refs 6, 7), Mad2 (refs 8, 9), Bub1 (refs 10, 11) and Bub3 (refs 12–14) indicates that fundamental aspects of the mitotic-checkpoint pathway may have been conserved throughout evolution. Nevertheless, the mitotic checkpoint in mammalian cells is more complex than in yeast, as exemplified by their requirement for two Bub1-related kinases instead of the single Bub1 kinase in yeast^{10,11,15}. Zw10 and Rod are kinetochore proteins that are required for faithful chromosome segregation in *Drosophila*^{16–19}.

Human Zw10 has been identified but its function was not examined²⁰. More recently, a putative human Rod complementary DNA has been reported but its authenticity was not verified¹⁹. To determine whether this cDNA encodes human Rod, we raised antibodies against the amino-terminal 809 residues of the 2,209-residue protein. Affinity-purified antibodies identified a single protein in lysates prepared from asynchronous and mitotic HeLa cells, the size of which was close to the calculated relative molecular mass of 250,000 (M_r 250K; Fig. 1, lanes 1 and 2). To confirm further that our antibodies recognized hRod, we relied on genetic evidence from *Drosophila* indicating Rod and Zw10 may be associated with each other^{18,20}. Indeed, an immunoprecipitate obtained with anti-hZw10 antibodies was found to contain hRod (Fig. 1, lane 3). Likewise, hRod immunoprecipitates were found to contain hZw10 (Fig. 1, lane 4).

Immunofluorescence staining of HeLa cells at various stages of mitosis revealed that hRod was concentrated at kinetochores during early and late stages of prometaphase (Fig. 2A, b and d). By metaphase, hRod was still detectable at kinetochores, but was also found along spindle fibres and prominently at the poles (Fig. 2A, f). By late anaphase, hRod was no longer detectable on kinetochores or along spindle fibres, but remained at the spindle poles (Fig. 2A, h). Prominent hRod staining was detected in the cytoplasm of all cells, indicating that only a fraction of the total pool of

hRod was associated with kinetochores and the spindle.

To determine the earliest time at which hRod can be detected at kinetochores, we co-stained cells with anti-centromere (ACA) and anti-hZw10 antibodies. In interphase cells, hRod was uniformly distributed throughout the cytoplasm and nucleus but did not co-localize with ACA (data not shown). By prophase, hRod was clearly present at kinetochores, as determined by co-localization with ACA (Fig. 2B, b and d). Interestingly, hZw10 was not detected at kinetochores at this time (Fig. 2B, c). By prometaphase, hRod and hZw10 were co-localized at kinetochores (Fig. 2B, e–h).

We examined the *in vivo* functions of hRod and hZw10 by micro-injecting affinity-purified antibodies against these proteins into synchronized HeLa cells shortly after their release from the G1/S boundary. Injection of either anti-hRod or anti-hZw10 antibodies prevented the assembly of hRod, hZw10, and of the p150^{glued} subunit of the dynactin complex²¹ onto kinetochores of mitotic chromosomes (see Supplementary Information). Kinetochore localization of hZw10, hRod and p150^{glued} was unaffected in cells that were injected with equivalent amounts of non-immune immunoglobulin G (IgG; see Supplementary Information). Antibodies against hZw10 and hROD did not prevent binding of hZw10, hRod and p150^{glued} to kinetochores by grossly disrupting

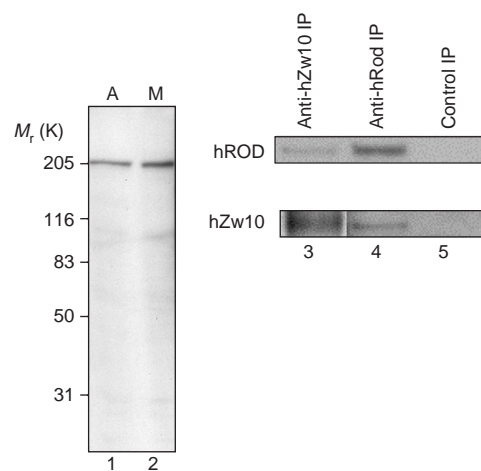


Figure 1 hROD and hZw10 form a complex *in vivo*. Cell extracts prepared from asynchronous (lane 1) and mitotic (lane 2) HeLa cells were probed with anti-hRod antibodies. Immunoprecipitates (IP) of hZw10 (lane 3), hRod (lane 4), and non-immune antibodies (lane 5) were probed with anti-hRod and anti-hZw10 antibodies.

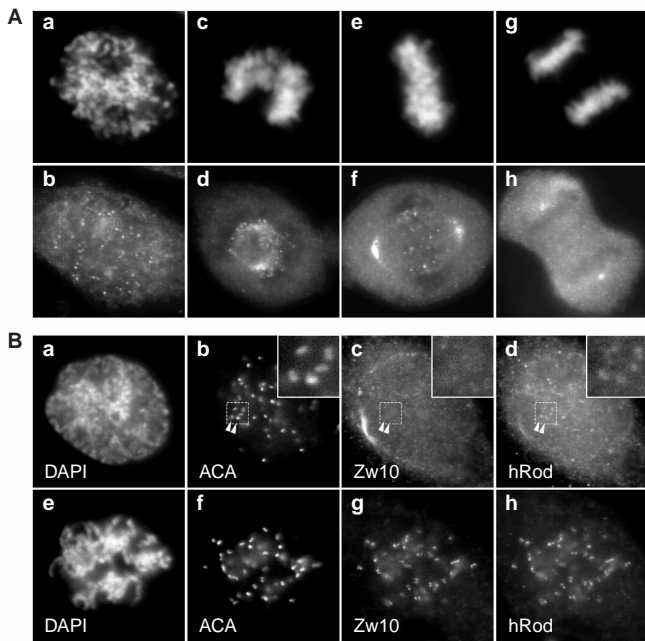


Figure 2 Localization of hRod during mitosis. **A**, Immunofluorescence staining of HeLa cells with anti-hRod antibodies during early prometaphase (**a**, **b**), late prometaphase (**c**, **d**), metaphase (**e**, **f**) and late anaphase (**g**, **h**). **B**, Triple staining with anti-hRod, anti-hZw10 and ACA antibodies in prophase (**a–d**) and prometaphase (**e–h**) HeLa cells. Insets in **b–d** are magnified views of the boxed area. Arrowheads indicate a pair of kinetochores that contain hRod but not hZw10. DNA was stained with DAPI (**a**, **e**).

kinetochore structure, as the CENP-E motor was able to assemble onto these kinetochores (see Supplementary Information).

The majority of the chromosomes in cells that were injected with either anti-hRod or anti-hZw10 antibodies appeared to be aligned at the spindle equator, although unaligned chromosomes were frequently seen (see Supplementary Information). If disruption of hZw10 and hRod functions interferes with chromosome alignment, we would expect the checkpoint to arrest cells in mitosis. When cells that were injected with anti-hRod and anti-hZw10 antibodies were examined 16 h after their release from the G1/S boundary, most had divided instead of accumulating in mitosis (Fig. 3A). However, the presence of chromatin bridges in between the divided cells (Fig. 3A, a and c) indicated that cell division was abnormal. This interpretation is supported by the fact that lagging chromosomes were seen in anaphase cells in which hZw10 and hRod functions were disrupted (Fig. 3A, e).

Chromatin bridges and lagging chromosomes are frequently seen in cells that lack the mitotic checkpoint because these cells divide in the presence of unaligned chromosomes¹⁵. We therefore investigated whether cells with defective hRod and hZw10 functions could arrest in mitosis in the presence of microtubule inhibitors (Fig. 3B). We injected synchronized cells with anti-hRod or anti-hZw10 antibodies and then added nocodazole several hours before they entered mitosis. Examination of the injected cells that reached mitosis showed that hRod and hZw10 were absent from kinetochores (data not shown). At 16 h after release from the G1/S boundary, uninjected cells and cells injected with non-immune IgG were arrested in mitosis after nocodazole treatment (Fig. 3C). In contrast, cells injected with either anti-hRod or anti-hZw10 antibodies exited mitosis without dividing (Fig. 3C) and formed highly aberrant nuclei that were probably polyploid (Fig. 3B, a–f).

We next examined whether the loss of hZw10 and hRod from

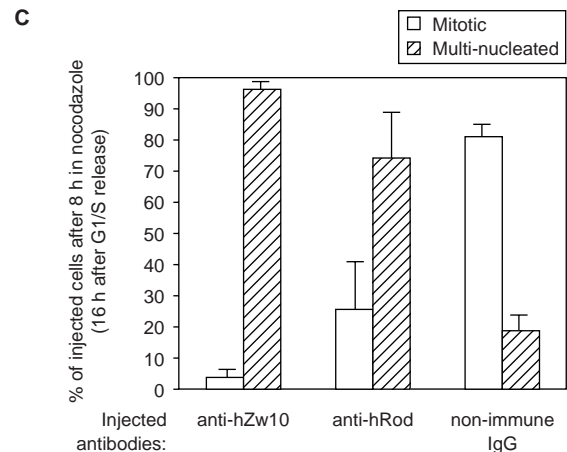
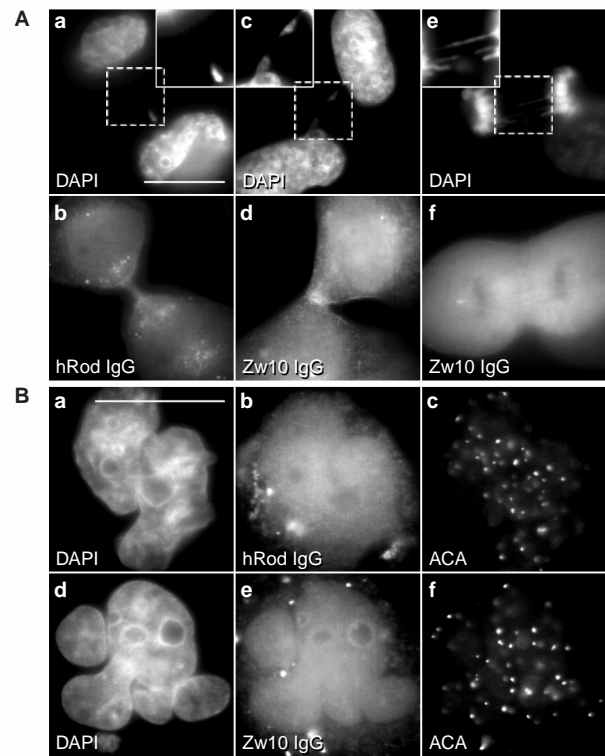


Figure 3 hRod and hZw10 are essential components of the mitotic checkpoint. **A**, HeLa cells synchronized at the G1/S boundary were injected with anti-hRod or anti-hZw10 antibodies shortly after release from the block. After 16 h, injected cells divided with chromatin bridges stretched between them (**a–d**). Lagging chromosomes are visible in an anaphase cell that was injected with anti-hZw10 antibodies (**e**, **f**). Injected antibodies were stained as described; DNA was stained with DAPI (**a**, **c**, **e**). Insets in **a**, **c**, **e** show magnified views of the boxed regions. **B**, HeLa cells injected with anti-hRod or anti-hZw10 antibodies were exposed to nocodazole and examined 16 h after release from the G1/S boundary. Scale bars represent 10 μ m. **C**, Comparison of the fates of HeLa cells injected with anti-hZw10, anti-hRod or non-immune antibodies after exposure to nocodazole. Synchronized HeLa cells were injected within 2 h of release from the G1/S boundary; nocodazole was added 8 h after release. HeLa cells normally enter mitosis 10–12 h after release. The histogram compares the mitotic (open bars), and multi-nucleated (striped bars) indices of cells injected with anti-hZw10, anti-hRod and non-immune antibodies 16 h after release from the G1/S boundary. For each experiment, 80–120 injected cells were counted; Values are means \pm s.d. from three independent experiments.

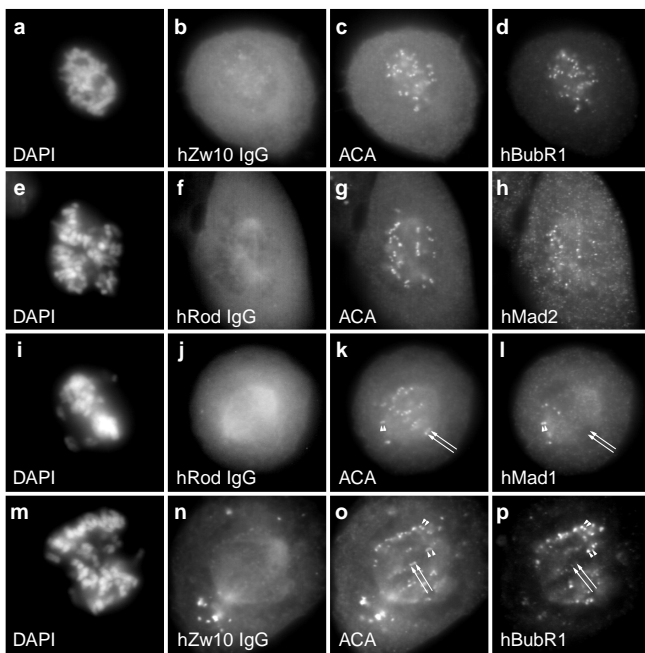


Figure 4 hRod and hZw10 are not required for other checkpoint proteins to bind to kinetochores. Anti-hRod and anti-hZw10 antibodies were injected into synchronized HeLa cells (**b, f, j, n**) and then stained with antibodies against various checkpoint proteins and with ACA after cells entered mitosis. DNA was stained with DAPI (**a, e, i, m**). **a–d**, Nocodazole-treated mitotic cell, showing hBubR1 at its kinetochores. **e–h**, Prometaphase cell that was not treated with drugs, showing hMad2 (**e**) at kinetochores. **i–l**, hMad1 can localize to unattached (arrowheads) but not to attached (arrows) kinetochores. **m–p**, hBubR1 preferentially localizes to unattached (arrowheads) over attached (arrows) kinetochores.

kinetochores affects the ability of other checkpoint proteins to bind to kinetochores. Kinetochores depleted in hZw10 and hRod retained hBubR1 kinase in a mitotic cell that was exposed to nocodazole (Fig. 4a–d). Loss of hRod and hZw10 from kinetochores also did not affect the ability of Mad1 or Mad2 to bind to kinetochores in mitotic cells that were not treated with nocodazole (Fig. 4e–l). In these cells, prominent Mad1 staining was observed at the kinetochores of chromosomes that had not reached the spindle equator, whereas kinetochores located within the central spindle, which were thus more likely to have established bipolar attachments, exhibited no detectable levels of Mad1 (Fig. 4l). Similarly, hBubR1 kinase accumulated to higher levels at the kinetochores of unaligned chromosomes (Fig. 4p, arrowheads) over those that appeared to be aligned at the centre of the cell (Fig. 4p, arrows) despite the loss of hZw10 and hRod from kinetochores. Unlike Mad1 and Mad2, hBubR1 does not completely dissociate from kinetochores even after they are aligned²².

We have examined the *in vivo* functions of the kinetochore proteins hRod and hZw10 and found that these proteins depend on each other for stable association with the kinetochore. In addition, these proteins are required for the assembly of the dynein–dynactin complex onto kinetochores. These results are fully consistent with those reported for *Drosophila* Zw10 and Rod^{18,23}. The molecular basis of how the dynein–dynactin complexes are recruited to kinetochores is not clear, but an interaction between hZw10 and the dynamitin subunit of the dynactin complex has been detected by yeast two-hybrid assay²⁰.

The majority of chromosomes that lacked hRod, hZw10 and

p150^{glued} at their kinetochores seemed to have reached metaphase alignment. This indicates that the presence of dynein–dynactin at kinetochores is not essential for chromosome alignment. This is consistent with the finding that chromosomes are able to align in Zw10- and Rod-mutant flies^{18–20}. The presence of CENP-E at kinetochores that were depleted in hRod, hZw10 and p150^{glued} indicates that this is likely to be the motor that is responsible for aligning the chromosomes^{24,25}. We have not examined whether these kinetochores retain the kinesin-like protein mitotic-centromere associated kinesin mitotic-centromere associated kinesin (MCAK)²⁶. Unlike those in *Drosophila*, not all chromosomes with kinetochores that were depleted of hRod, hZw10 and p150^{glued} were aligned. It is possible that dynein may enhance the efficiency with which kinetochores become attached to the spindle. This is supported by the observation that at the onset of mitosis, a kinetochore can make a lateral attachment to a single microtubule and be pulled polewards at a rate that is characteristic of dynein-mediated motion²⁷. When dynein is not present at kinetochores, chromosomes may not be efficiently pulled into the spindle. An alternative explanation for the lack of complete chromosome alignment is that cells depleted in these kinetochore components may exit mitosis prematurely.

Our results show that hRod and hZw10 are essential components of the mitotic checkpoint, as cells that were defective for hRod and hZw10 functions failed to arrest in mitosis when exposed to microtubule-depolymerizing drugs. hRod and hZw10 also seem to provide checkpoint functions that are important for normal mitotic progression, as cells divided with lagging chromosomes when hZw10 and hRod functions were disrupted. If disruption of hRod and hZw10 accelerated cells out of mitosis, as has been reported for Bub1 and Mad2 (refs 9, 10, 28), there may have been insufficient time for chromosomes to align before cells began to divide. Our findings are fully consistent with those described in the accompanying paper by Basto *et al.*²⁹, who showed that *Drosophila* Zw10 and Rod are new components of the spindle-assembly checkpoint. In their study, cells in *zw10* and *rod* mutants failed to accumulate in mitosis in the presence of colchicine. Mutant flies were found to degrade cyclin B prematurely and to separate their sister chromatids precociously, which can potentially explain the high incidence of aneuploidy.

We envision two ways in which hZw10 and hRod might provide checkpoint functions at kinetochores. It is possible that kinetochores lacking hZw10 and hRod failed to generate the signal to block mitotic exit even though chromosomes were unaligned. However, the loss of hZw10 and hRod from kinetochores did not affect the ability of the checkpoint proteins Mad1, Mad2 and hBubR1 to bind there. These results mirror findings in *Drosophila*, in which kinetochore localization of the Bub1 and Bub3 checkpoint proteins was found to not require Zw10 or Rod^{13,30}. Furthermore, we observed that unattached kinetochores exhibited higher levels of Mad1 and hBubR1 than kinetochores that appeared to have established bipolar attachments. Thus, neither hZw10 nor hRod is required by kinetochores to bind Mad1 and hBubR1, or to release these proteins in response to microtubule interactions. In this regard, hZw10 and hRod could represent a separate arm of the checkpoint pathway that acts independently of Mad1, Mad2 and hBubR1. To discriminate between these models, it will be interesting to determine whether hZw10 and hRod monitor kinetochore–microtubule interactions mediated by dynein–dynactin. We have previously shown that hBubR1 kinase can associate with the CENP-E kinetochore motor, and we proposed that the checkpoint function of hBubR1 is to monitor CENP-E activity at kinetochores¹⁵. Microtubule interactions that are specified by multiple kinetochore motors would require an elaborate checkpoint system, which may be achieved by assigning different checkpoint proteins to the different motors. This division of labour may have evolved to accommodate the increased complexity of metazoan kinetochores. □

Methods

Anti-hRod and anti-Zw10 antibodies.

Full length hRod cDNA (KIAA0166) was from the Kazusa cDNA Project (Kazusa DNA Research Institute, Chiba, Japan). cDNA encoding the N-terminal 809 residues was subcloned into pGEX-KT and the glutathione-S-transferase (GST)-fused protein was expressed in *Escherichia coli* JM109. Purified fusion protein was used to immunize rats. Rabbit antibodies against hZw10 were raised against a GST-hZw10 fusion protein as described²⁰. For affinity purification, immune serum from hRod-injected rats or hZw10-injected rabbits was first incubated with Affi-gel (BioRad) that was coupled with a bacterial lysate that contained GST, in order to remove antibodies against GST and other bacterial proteins. The pre-adsorbed serum was then incubated overnight at 4 °C with Affi-gel 10 that was coupled with either GST-hRod or GST-hZw10. The columns were washed extensively with TBS-500 (10 mM Tris-HCl, pH7.4, and 500 mM NaCl). Antibodies were eluted with 0.5% acetic acid and 500 mM NaCl and immediately neutralized with 1 M Tris pH9.0. Fractions were monitored by light absorbance at 280 nm and the peak fractions were pooled, desalted and concentrated into 0.5 × PBS/50% glycerol. Antibodies to be used for micro-injections were concentrated to ~5 mg ml⁻¹ in Ca²⁺- and Mg²⁺-free PBS (Gibco), aliquoted and frozen at -80 °C.

Cell culture.

HeLa cells were grown in DMEM supplemented with 10% FBS in the presence of antibiotics in a humidified incubator at 37 °C. Cell synchronization was achieved by a double-thymidine block.

Immunofluorescence and micro-injections.

Cells used for immunofluorescence staining or for micro-injections were plated onto no. 1 glass coverslips and used 2–3 days later. For staining, cells were pre-extracted in KB (20 mM Tris-HCl pH7.5, 150 mM NaCl and 0.1% BSA) plus 0.2% Triton X-100 for 2 min at room temperature, fixed for 7 min in freshly prepared 3.5% paraformaldehyde/PBS pH 7.0 and rinsed in KB. Primary and secondary antibodies were diluted in KB and added to coverslips for 30–60 min at 37 °C in a humidified chamber. Rabbit anti-p150^{hbs1} and anti-Mad2 antibodies and human anti-centromere auto-antibodies (ACA) were gifts from R. Vallee (Univ. Massachusetts), E. D. Salmon (Univ. N. Carolina) and K. F. Sullivan (Scripps Institute), respectively. Anti-human Mad1 antibodies were provided by M. S. Campbell (Fox Chase Cancer Center, Philadelphia). Antibodies against CENP-E, hBubR1, hRod, hZw10 and hSMad1 were used at a final concentration of 0.5–1 µg ml⁻¹. Secondary antibodies conjugated to Alexa Fluor 488 (Molecular Probes), Texas Red and Cy5 (Jackson ImmunoResearch) were all used at 2 µg ml⁻¹.

For micro-injections, HeLa cells blocked at the G1/S boundary were washed and released into HEPES-buffered DMEM plus 10% FBS and returned to the incubator. Roughly 1 h after release, antibodies were injected into the nuclei of cells using an Eppendorf semi-automated micro-injector and Femtotip needles (Brinkmann Instruments Inc., Westbury, New York). Injections were administered using a Nikon TE300 inverted microscope. Injected cells were returned to the incubator and then fixed at a later time. Typically, mock- or non-immune-IgG-injected cells enter mitosis 9–10 h after release from the G1/S block. In cases in which injected cells were tested for their response to spindle damage, nocodazole (50 ng ml⁻¹) was added ~7 h after release from the G1/S boundary. Injected cells were identified by staining with the appropriate secondary antibodies.

Western blotting and immunoprecipitation.

HeLa cells were lysed with 1% NP40 lysis buffer (50 mM Tris pH 7.5, 150 mM NaCl, 1 mM dithiothreitol) with protease and phosphatase inhibitors (10 µg ml⁻¹ AEBSEF, 10 µg ml⁻¹ leupeptin, 5 µg ml⁻¹ pepstatin, 5 µg ml⁻¹ chymostatin, 10 µg ml⁻¹ aprotinin, 10 mM NaF, 1 mM Na₂VO₄, 60 mM β-glycerophosphate and 100 nM microcystin), and insoluble material was pelleted at 10,000g. Protein concentration of the lysates was determined by the BCA protein assay (Pierce Chemical Co., Rockford, Illinois). Lysates in 1 × SDS sample buffer were separated by 4–12% gradient SDS-PAGE; proteins were then transferred onto Immobilon-P membrane (Millipore, Bedford, Massachusetts) and probed with the appropriate antibodies. Primary antibodies were detected with alkaline phosphatase-conjugated anti-rabbit or anti-rat secondary antibodies used at 1:30,000 (Sigma) and then processed for

chemiluminescence detection using CPD-Star (Tropix, Bedford, Massachusetts). Immunoprecipitation was carried out with 300 µg of lysate; the final concentration of hRod and hZw10 antibody was ~2 µg ml⁻¹. Rabbit and rat antibodies were precipitated from lysates with protein A- and protein G-sepharose (Repligen, Cambridge, Massachusetts), respectively.

RECEIVED 21 JUNE 2000; REVISED 13 JULY 2000; ACCEPTED 8 AUGUST 2000; PUBLISHED 14 NOVEMBER 2000.

- Nicklas, R. B. *Science* **275**, 632–637 (1997).
- Rieder, C. L., Schultz, A., Cole, R. & Sluder, G. *J. Cell Biol.* **127**, 1301–1310 (1994).
- Li, R. & Murray, A. W. *Cell* **66**, 519–531 (1991).
- Hoyt, M. A., Totis, L. & Roberts, B. T. *Cell* **66**, 507–517 (1991).
- Weiss, E. & Winey, M. *J. Cell Biol.* **132**, 111–123 (1996).
- Jin, D. Y., Spencer, F. & Jeang, K. T. *Cell* **93**, 81–91 (1998).
- Chen, R. H., Shevchenko, A., Mann, M. & Murray, A. W. *J. Cell Biol.* **143**, 283–295 (1998).
- Li, Y. & Benezra, R. *Science* **274**, 246–248 (1996).
- Chen, R. H., Waters, J. C., Salmon, E. D. & Murray, A. W. *Science* **274**, 242–246 (1996).
- Taylor, S. S. & McKeon, F. *Cell* **89**, 727–735 (1997).
- Cahill, D. P. *et al.* *Nature* **392**, 300–303 (1998).
- Taylor, S. S., Ha, E. & McKeon, F. *J. Cell Biol.* **142**, 1–11 (1998).
- Martinez-Exposito, M. J., Kaplan, K. B., Copeland, J. & Sorger, P. K. *Proc. Natl Acad. Sci. USA* **96**, 8493–8498 (1999).
- Basu, J. *et al.* *Chromosoma* **107**, 376–385 (1998).
- Chan, G. K. T., Jablonski, S. A., Sudakin, V., Hittle, J. C. & Yen, T. J. *J. Cell Biol.* **146**, 941–954 (1999).
- Karess, R. E. & Glover, D. M. *J. Cell Biol.* **109**, 2951–2961 (1989).
- Williams, B. C., Karr, T. L., Montgomery, J. M. & Goldberg, M. L. *J. Cell Biol.* **118**, 759–773 (1992).
- Williams, B. C., Gatti, M. & Goldberg, M. L. *J. Cell Biol.* **134**, 1127–1140 (1996).
- Scaerou, F. *et al.* *J. Cell Sci.* **112**, 3757–3768 (1999).
- Starr, D. A. *et al.* *J. Cell Biol.* **138**, 1289–1301 (1997).
- Holzbaun, E. L. *et al.* *Nature* **351**, 579–583 (1991).
- Jablonski, S. A., Chan, G. K. T., Cooke, C. A., Earnshaw, W. C. & Yen, T. J. *Chromosoma* **107**, 386–396 (1998).
- Starr, D. A., Williams, B. C., Hays, T. S. & Goldberg, M. L. *J. Cell Biol.* **142**, 763–774 (1998).
- Schaar, B. T., Chan, G. K. T., Maddox, P., Salmon, E. D. & Yen, T. J. *J. Cell Biol.* **139**, 1373–1382 (1997).
- Wood, K. W., Sakowicz, R., Goldstein, L. S. & Cleveland, D. W. *Cell* **91**, 357–366 (1997).
- Wordeman, L. & Mitchison, T. J. *J. Cell Biol.* **128**, 95–104 (1995).
- Rieder, C. L. & Alexander, S. P. *J. Cell Biol.* **110**, 81–95 (1990).
- G. J., Chen, R. H. & Murray, A. W. *J. Cell Biol.* **141**, 1193–1205 (1998).
- Basto, R., Gomes, R. & Karess, R. E. Rough deal and Zw10 are required for the metaphase checkpoint in *Drosophila*. *Nature Cell Biol.* **2**, 939–943 (2000).
- Basu, J. *et al.* *J. Cell Biol.* **146**, 13–28 (1999).
- Campbell, M. S. & Yen, T. J. Mitotic-checkpoint proteins HsMad1 and HsMad2 are associated with nuclear-pore complexes in interphase (submitted).

ACKNOWLEDGEMENT

We thank J. C. Hittle and H. L. Simpkins for micro-injections and for purifying hZw10 antibodies, respectively. We also thank all members of the Yen laboratory for comments and suggestions during the course of the work. This work was supported by grants to T.J.Y. from the NIH, ACS, and Leukemia and Lymphoma Society, core grant CA06927 and an appropriation from the Commonwealth of Pennsylvania. M.L.G. was supported by a grant from the NIH. Correspondence and requests for materials should be addressed to T.J.Y. Supplementary Information is available on *Nature Cell Biology's* website (<http://cellbio.nature.com>) or as paper copy from the London editorial office of *Nature Cell Biology*.

Erratum

In Fig. 4l, the antibody used was against hMad1 and not hMad2 as stated.

Ref. 28 should be as follows: Gorbisky, G. J., Chen, R. H. & Murray, A. W. *J. Cell Biol.* **110**, 81–95 (1998).

Ref. 31 is cited in the Methods, “Immunofluorescence and micro-injections”, line 8 as M. S. Campbell (Fox Chase Cancer Centre, Philadelphia).

For corrected version please see the print version of *Nature Cell Biology* vol. 2, no. 12, December 2000.

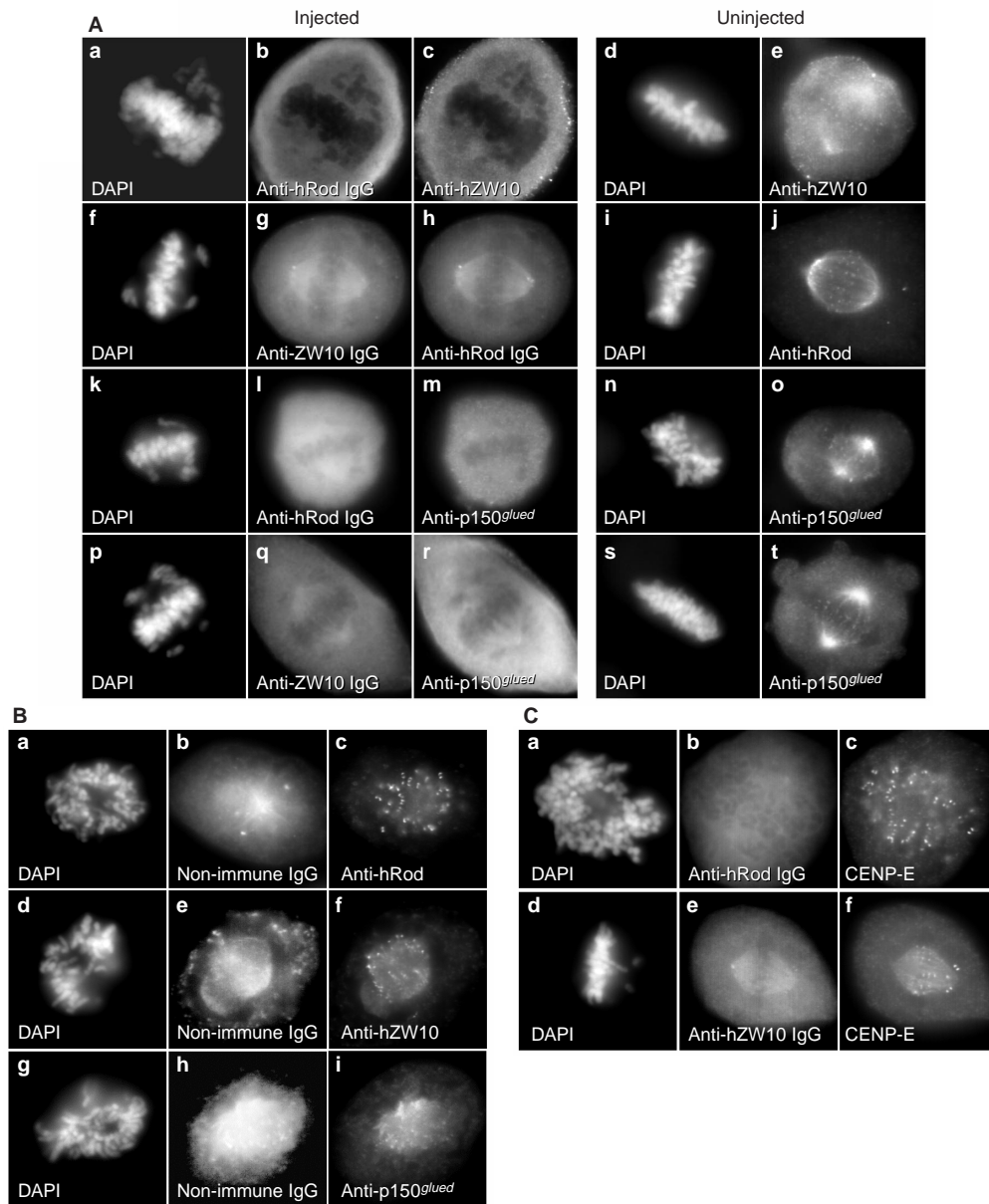


Figure S1 Characterization of kinetochores depleted in hRod and hZW10. A, HeLa cells released from the G1/S boundary were injected with anti-hRod or anti-hZW10 antibodies and sampled when they entered mitosis. DNA was stained with DAPI (a, d, f, i, k, n, p, s). Cells were stained for injected anti-hROD (b, l) or anti-hZW10 immunoglobulin G (IgG; g, q) or endogenous hZW10 (c, e), hRod (h, j) or p150^{glued} (m, o, r, t). Exposure times were identical between injected and uninjected cells. Cells were fixed to prevent injected IgG from being extracted during subsequent permeabilization; this contributed to higher levels of cytosolic staining and diffuse spindle staining in many cases. B, HeLa cells injected with non-immune rab-

bit IgG (b) or rat IgG (e, h) that had entered prometaphase were stained with the appropriate Cy5-conjugated secondary antibody to visualize the injected antibodies (b, e, h) and co-stained with either rat anti-hRod (c), rabbit anti-hZW10 (f) or rabbit anti-p150^{glued} (i) antibodies to visualize endogenous protein. DNA was stained with DAPI (a, d, g). C, CENP-E is present at kinetochores that are depleted in hRod and hZW10. HeLa cells were stained for the injected rat anti-hRod (b) or rabbit anti-hZW10 (e) antibodies as described above and then co-stained with rabbit anti-CENP-E (c) and rat anti-CENP-E (f) antibodies. DNA was stained with DAPI (a, d).